Supplementary tables

Table 1S – Notations of parameters used in the paper and in the original models

Parameters notation in the paper	Parameters notation by Bentele *et al.*, 2004
f_{degr}	f_{degrad}
k_{Apop}	$k\_Apoptosome$
k_d	K_DEGRAD
k_{dd}	$K\_DEGRAD\_deathSub$
k_{ds}	K_DEGRAD_steady
k_{DISC_FLIP}	k_DISC_FLIP
k_{DISC_pro8}	$k\_DISC\_procas8$
k_{DFp8}	$k\_DISC\_FLIP\_to\_cas8\_IM$
k_{LR}	k_LR
k_{32}	$k\_cas\_3\_2$
k_{36}	$k\_cas\_3\_6$
k_{38}	$0.145 \cdot k\_cas\_6\_8$
k_{68}	$k\_cas\_6\_8$
k_{78}	$k\_cas\_8\_7$
k_{83}	$k\_cas\_8\_3$
k_{3act}	$0.18 \cdot k\_cas7\_apop\_activity$
k_{36act}	$k\_cas36\_apop\_activity$
k_{39IAP}	k_cas39_IAP
k_{7act}	$k\_cas7\_apop\_activity$
k_{8Bid}	k_cas8_Bid
Km_{32}	$Km\_cas\_3\_2$
Km_{36}	$Km\_cas\_3\_69$
Km_{367act}	$Km\_cas367\_apop\_activity$
Km_{38}	$Km\_cas\_6\_8$
Km_{68}	$Km\_cas\_6\_8$
Km_{78}	$Km\_cas\_8\_7$
Km_{8Bid}	Km_cas28_Bid
Km_{893}	$Km\_cas\_89\_3$
x_{aa}	$x_{apop\ activity}$
Parameters notation in the paper	**Parameters notation by Neumann *et al.*, 2004**
$k_{p43-FLIP\_IKK}$	$k13$

Table 2S – Table of all reactions (excepting degradation) and rate constants in the composite model

№	Reactions	Kinetic laws	Rate constants (nM^{-1}min^{-1}; min^{-1})	Comments[1]
nr1	CD95L + CD95R:FADD → DISC	$n_{k1} \cdot C_{CD95L} \cdot C_{CD95R}$	1.0	$k1$, Neumann *et al.*, 2010
nr2	pro8 + DISC → DISC:pro8	$n_{k2} \cdot C_{DISC} \cdot C_{pro8}$	$1.277248E - 4$	$k2$, Neumann *et al.*, 2010
nr3	DISC + FLIPL → DISC:FLIPL	$n_{k3} \cdot C_{DISC} \cdot C_{FLIPL}$	0.6693316	$k3$, Neumann *et al.*, 2010
nr5	DISC:pro8 + pro8 → 2 x p43p41	$n_{k5} \cdot C_{DISC:pro8} \cdot C_{pro8}$	$5.946569E - 4$	$k5$, Neumann *et al.*, 2010
nr6	DISC:pro8 + FLIPL → p43-FLIP	$n_{k6} \cdot C_{DISC:pro8} \cdot C_{FLIPL}$	0.9999999	$k6$, Neumann *et al.*, 2010
nr7	DISC:pro8 + FLIPS → DISC:pro8:FLIPS	$n_{k7} \cdot C_{DISC:pro8} \cdot C_{FLIPS}$	0.8875063	$k7$, Neumann *et al.*, 2010
nr8	DISC:FLIPL + pro8 → p43FLIP	$n_{k5} \cdot C_{DISC:FLIPL} \cdot C_{pro8}$	$5.946569E - 4$	$k5$, Neumann *et al.*, 2010
nr9	DISC:FLIPL + FLIPL → DISC:FLIPL$_2$	$n_{k6} \cdot C_{DISC:FLIPL} \cdot C_{FLIPL}$	0.9999999	$k6$, Neumann *et al.*, 2010
nr10	DISC:FLIPL + FLIPS → DISC:FLIPL:FLIPS	$n_{k7} \cdot C_{DISC:FLIPL} \cdot C_{FLIPS}$	0.8875063	$k7$, Neumann *et al.*, 2010
nr14	2 x p43p41 → casp8	$n_{k8} \cdot C_{p43p41}^{2}$	$8.044378E - 4$	$k8$, Neumann *et al.*, 2010
nr15_m	pro3 –casp9→ casp3	$n_{k9} \cdot C_{casp9} \cdot C_{pro3}$	0.04920673	**Fitted value**, $k9 = 0.002249759$, Neumann *et al.*, 2010
nr16	pro8 -casp3→ p43p41	$n_{k10} \cdot C_{pro8} \cdot C_{casp3}$	0.01205258	**Fitted value**, $k10 = 0.1205258$, Neumann *et al.*, 2010
nr19	p43FLIP → p43-FLIP:IKK*	$n_{k13} \cdot IKK_0 \cdot C_{p43FLIP}$	$n_{k13} = 7.20426E - 4$, $IKK_0 = 5.772825$	$k13$, $C_{IKK}(0)$, Neumann *et al.*, 2010
nr20	NF-κB:IκB -p43-FLIP:IKK→ NF-κB:IκB-P	$n_{k14} \cdot C_{NF\kappa B:I\kappa B} \cdot C_{p43FLIP:IKK^*}$	0.3588224	$k14$, Neumann *et al.*, 2010
nr21	NF-κB:IκB-P → NF-κB*	$n_{k15} \cdot C_{NF\kappa B:I\kappa BP}$	3.684162	$k15$, Neumann *et al.*, 2010
br6*_m	pro9 -tBid→ casp9	$b_{k6} \cdot C_{tBid} \cdot C_{pro9}$	0.06310456	–
br7*	Bid -casp8→ tBid	$b_{k7} \cdot C_{casp8} \cdot C_{Bid}$	$6.0004E - 4$	**Fitted value**, $k_{8Bid}/Km_{8Bid} = 5.3325E - 4$, the reduced Bentele's model
br8*	pro2 -casp3→ (cleavage)	$\dfrac{b_{k8} \cdot C_{casp3} \cdot C_{pro2}}{b_{Km8} + C_{pro2}}$	$b_{k8} = 15.63123994$, $b_{Km8} = 55.57400642$	**Fitted values**, $k_{32} = 0.18137$, $Km_{32} = 55.574$, Bentele *et al.*, 2004
br9*	pro3 -casp8→ casp3	$\dfrac{b_{k9} \cdot C_{casp8} \cdot C_{pro3}}{b_{Km9} + C_{pro3}}$	$b_{k9} = 0.0$ (HeLa) or 0.27246 (SKW 6.4), $b_{Km9} = 1.03542544$	**Fitted values**, $k_{83} = 1.90358$, $Km_{893} = 89.02911547$, Bentele *et al.*, 2004
br10*	pro7 -casp8→ (cleavage)	$b_{k10} \cdot C_{casp8} \cdot C_{pro7}$	10.89517864	**Fitted value**, $k_{78}/Km_{78} = 0.01016$, the reduced Bentele's model
br11*	PARP –casp3→ cPARP	$b_{k11} \cdot C_{casp7} \cdot C_{PARP}$	73.49560485	**Fitted value**, $0.18 \cdot k_{7act}/Km_{367act} = 0.00824$, the reduced Bentele's model
br12*	casp3 + IAP → (inhibition)	$b_{k12} \cdot C_{casp3} \cdot C_{IAP}$	0.01	**Fitted value**, $k_{39IAP} = 45824.409 \cdot 5 \cdot 10^{-5}$, Bentele *et al.*, 2004
br13*	-casp3→ Apoptotic activity	$b_{k13} \cdot (1.0 - x_{aa}) \cdot C_{casp3}$	5956.81008868	**Fitted value**, $(k_{36act} + 0.18 \cdot k_{7act})/Km_{367act} = 0.01053$, Bentele et al., 2004

---

[1] The column contains basic parameters or expressions (and their values if they were refitted) in the combined models.

Table 3S – Table of degraded species and kinetic laws of degradation in the composite model

Degraded species	Degradation rates	Rate constants (min^{-1})
pro2, pro3, pro8, DISC:pro8, DISC:pro8:FLIPS, pro9, Bid, PARP	$f_{degr} = degr \cdot x_{aa}^2$	$degr = \begin{cases} 0.0, & \text{HeLa cells,} \\ 0.0542, & \text{SKW 6.4 cells,} \quad C_{CD95L} = 5\,\mu g/ml, \\ 0.0084, & \text{SKW 6.4 cells,} \quad C_{CD95L} = 200\,ng/ml, \\ 0.0028, & \text{SKW 6.4 cells,} \quad 1\,ng/ml \le C_{CD95L} \le 100\,ng/ml. \end{cases}$
casp3	$f_{degr} = degr \cdot x_{aa}^2 + n_{k12}$	$n_{k12} = 0.1502914$, ($k12$, Neumann *et al.*, 2010)
casp8	$f_{degr} = degr \cdot x_{aa}^2 + n_{k11}$	$n_{k11} = 0.02891451$, ($k11$, Neumann *et al.*, 2010)
casp9	$f_{degr} = degr \cdot x_{aa}^2 + degr_{casp9}$	$degr_{casp9} = 0.10025628$
cPARP	$f_{degr} = degr_{cPARP}$	0.01748, (K_DEGRAD_PARP, Bentele *et al.*, 2004)
tBid	$f_{degr} = degr_{tBid}$	0.04999612
p43-FLIP:IKK*	$f_{degr} = n_{k16}$	0.02229912, ($k16$, Neumann *et al.*, 2010)
Apoptotic activity (x_{aa})	$degr_{apop\ activity}$	0.00219407

Table 4S – Table of nonzero initial concentrations in the composite model

Species	Initial concentrations (nM)			
	Neumann *et al.*, 2010 HeLa cells	Bentele *et al.*, 2004 SKW 6.4 cells	Composite model HeLa cells	Composite model SKW 6.4 cells
CD95L	113.22, 37.74, 18.87	1990.0, 79.6	113.22, 37.74, 18.87	1990.0, 79.6
CD95R	–	442.820768294033	–	–
CD95R:FADD	91.26592	0.0	91.26592	611.6891578799691
procaspase-2	–	157.644193512676	157.644193512676	157.644193512676
procaspase-3	1.443404	112.45433410827	14.43404	2.3438636537313413
procaspase-7	–	18.7933134063988	18.7933134063988	18.7933134063988
procaspase-8	64.47652	442.820768294033	64.47652	350.0248656584318
procaspase-9	–	245.101295250747	2.9090736162783806	245.101295250747
FLIPL	7.398562	65.0213661020702	7.398562	7.398562
FLIPS	5.083923	65.0213661020702	5.083923	70.44906883596883
IAP	–	12.2160965349275	1.221610	1.221610
Bid	–	231.760433964353	5.003142624870996	231.760433964353
IKK	5.772825	–	5.772825	5.772825
NF-κB:IκB	4.739546	–	4.739546	4.739546
PARP	–	11.1615188752353	11.1615188752353	11.1615188752353

Table 5S – Steady state analysis of the Bentele's model and the composite model

Species	Steady state values, anti-CD95 = 200 ng/ml			Steady state values, anti-CD95 = 5 μg/ml		
	Original model	Reduced model	Composite model	Original model	Reduced model	Composite model
procaspase-2	0.0000374	0.0000316	2.4468579	0.0013440	0.0013602	0.0000096
procaspase-3	–	–	–	0.0	0.0	0.0
procaspase-7	–	–	–	0.0	0.0	0.0
procaspase-8	25.1700455	27.2240392	14.9514288 (total value)	0.0000016	0.0	0.0000367 (total value)
procaspase-9	0.0	0.0	0.0	–	–	–
caspase-8	0.0	0.0	0.0	0.0	0.0	0.0
p43/p41	0.0	0.0	0.0001051	–	–	–
Bid	–	–	–	0.0411840	0.0342991	0.0000298
tBid	–	–	–	0.0901602	0.1040935	0.0
PARP	0.0	0.0	0.0	0.0	0.0	0.0
cPARP	–	–	–	0.0	0.0	0.0

Table 6S – Steady state analysis of the Neumann's model and the composite model

Species	Steady state values, anti-CD95 = 1500 ng/ml			Steady state values, anti-CD95 = 500 ng/ml			Steady state values, anti-CD95 = 250 ng/ml		
	Original model	Reduced model	Composite model	Original model	Reduced model	Composite model	Original model	Reduced model	Composite model
procaspase-8 (total)	12.0752771	12.0751903	12.0181928	2.6562426	2.6562649	2.3208092	9.6046242	9.6052138	13.2926881
p43/p41	0.0010204	0.0010204	0.0000891	0.0009555	0.0009555	0.0000948	0.0008922	0.0008922	0.0000883
caspase-8	0.0	0.0	0.0	0.0	0.0	0.0	0.0	0.0	0.0
procaspase-3	0.1992635	0.1992525	3.8521010	0.1350020	0.1349977	3.7249153	0.1721551	0.1721569	3.8516549
caspase-3	0.0	0.0	0.0	0.0	0.0	0.0	0.0	0.0	0.0
IκB	0.0	0.0	0.0	0.0000020	0.0000020	0.0000020	0.1519007	0.1526973	0.1526973
IκB-P	0.0	0.0	0.0	0.0	0.0	0.0	0.0	0.0	0.0
p43-FLIP	0.0	0.0	0.0	0.0	0.0	0.0	0.0	0.0	0.0

Table 7S – Calculation of the mean sensitivity for the investigated apoptosis models

Cell lines, anti-CD95 concentrations	The model by Bentele *et al.*			The model by Neumann *et al.*			The composite model, all parameters
	Original model		Reduced model	Original model		Reduced model	
	All parameters	Retained parameters		All parameters	Retained parameters		
SKW 6.4, 5 μg/ml	−34.49	−33.79	−29.72	–	–	–	−146.84
SKW 6.4, 200 ng/ml	−25.64	−24.95	−38.97	–	–	–	−114.13
HeLa, 1500 ng/ml	–	–	–	−30.71	−30.42	−30.29	−30.21
HeLa, 500 ng/ml	–	–	–	−79.85	−79.52	−78.94	−79.88
HeLa, 250 ng/ml	–	–	–	−88.05	−87.60	−88.70	−97.69

Table 8S – Analysis of predictions regarding apoptosis in HeLa cells as formulated by Neumann *et al*.

№[2]	Behavior of the model by Neumann *et al*.	Behavior of the reduced model	The composite model behavior	Predictions by Neumann *et al*.[3]
1*				The concentration of anti-CD95 required for the apoptosis induction (the apoptotic threshold), is within the range of 30-100 ng/ml. This range remains the same for CD95 decreased by about 12-fold. The simulation time, which we used to reproduce this prediction, was 60 hours.
2*				The decreased receptor number results in impairment of both CD95- and NF-κB-signaling pathways. To test this prediction, Neumann *et al*. considered levels of caspases-8 cleavage and IκB-α degradation for the original (solid lines) amount of CD95 and the amount decreased by about 12-fold (dashed lines). The concentration of anti-CD95 was 500 ng/ml.
3*				Along with increasing the concentration of anti-CD95 from 500 ng/ml to 1500 ng/ml, p43/p41 peaks earlier, while there is almost no difference for p43-FLIP.
4				Increased concentrations of cFLIPS inhibit both apoptotic and NF-κB pathways, although p43-FLIP generation is inhibited at a lower threshold than p43/p41 generation.

[2] All the predictions marked with an asterisk were experimentally tested by Neumann *et al*. and confirmed, unless otherwise noted.
[3] The The simulation time in predictions 3-7 was 360 min. The concentration of anti-CD95 considered by the authors in predictions 4-7 was 1000 ng/ml.
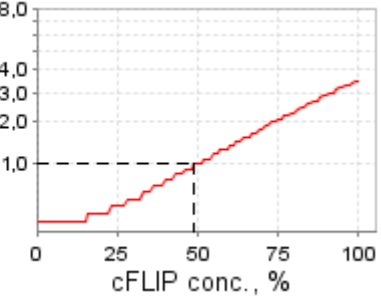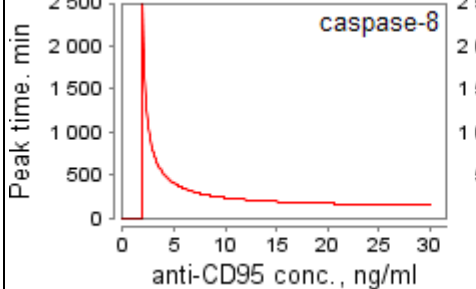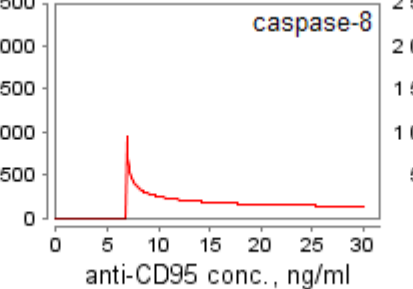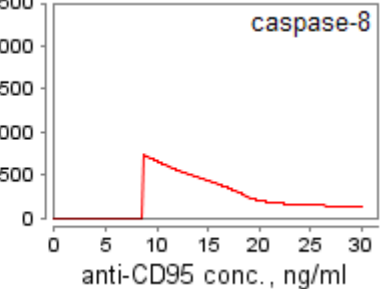
Table 8S (continuation)
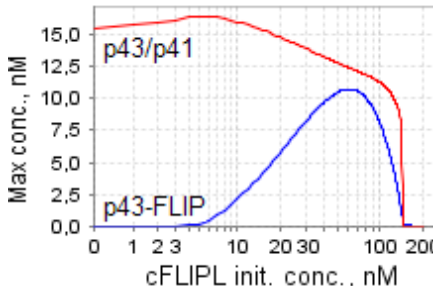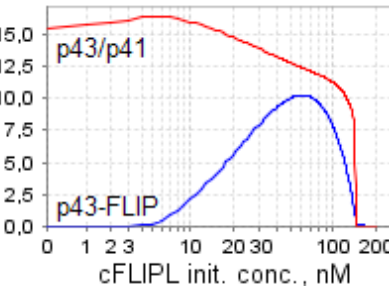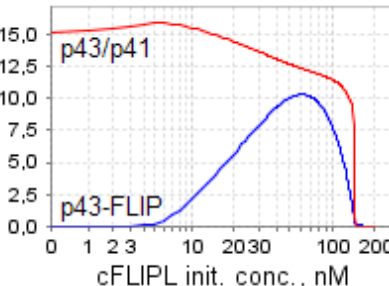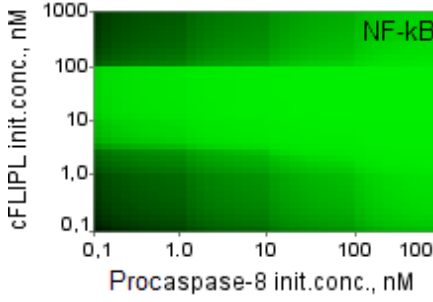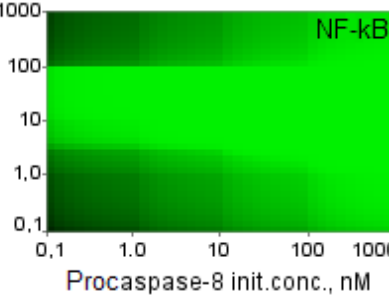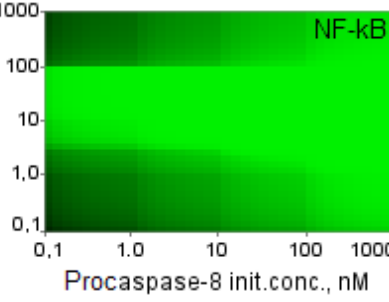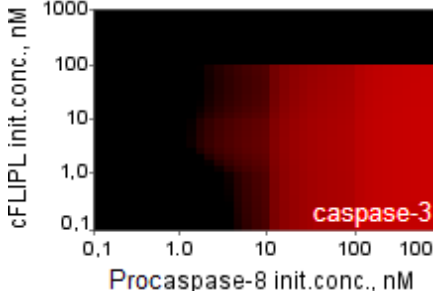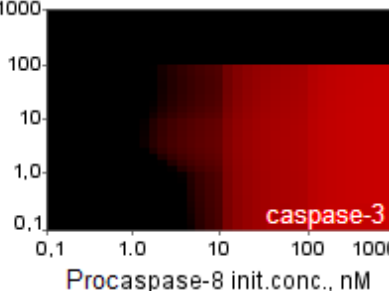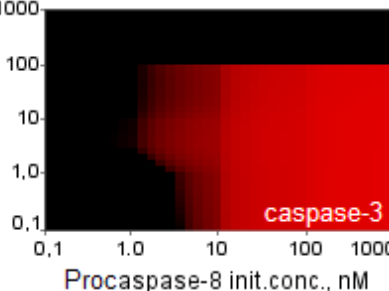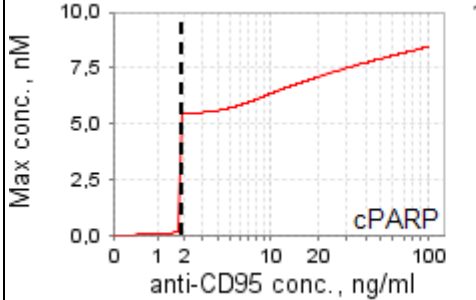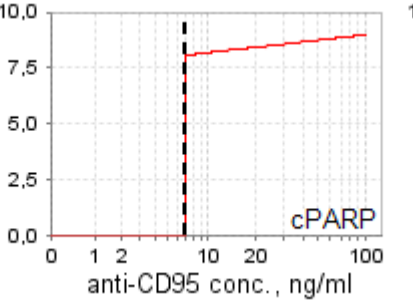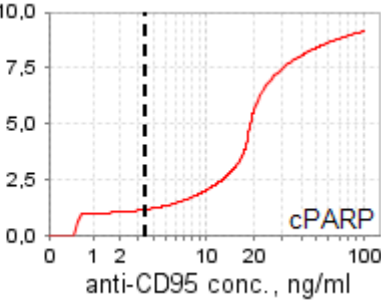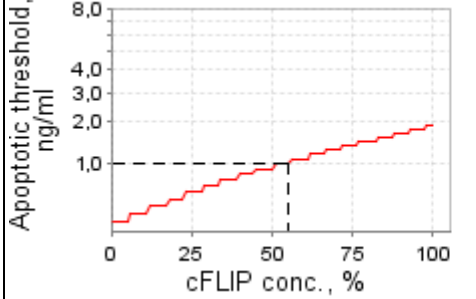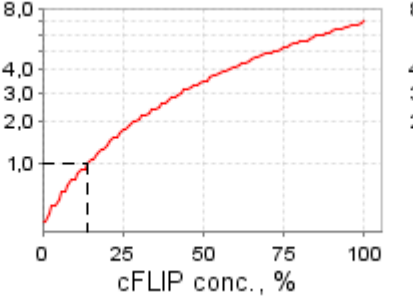
№	Behavior of the model by Neumann *et al.*	Behavior of the reduced model	The composite model behavior	Predictions by Neumann *et al.*
5*				Increasing the concentration of cFLIPL leads to a steep increase in p43-FLIP generation until it reaches a maximum, after which the curve drops. Lowered levels of cFLIPL result in very little p43-FLIP but almost unchanged levels of p43/p41. At very high concentrations of cFLIPL no p43-FLIP is generated. This drop-off was not observed experimentally by the authors.
6*				Only an intermediate level of cFLIPL promotes NF-kB activation. Decreased levels of procaspase-8 lead to a significantly lower amount of p43-FLIP and, subsequently, NF-κB. The figures show of logarithmic dependence of the maximal NF-κB concentration on the initial values of procaspase-8 and cFLIPL
7*				High cFLIPL or low procaspase-8 concentrations cause suppression of apoptosis. The figures show the same dependence as considered in the previous prediction, but with caspases-3 instead of NF-κB.

Table 9S – Predictions of the models for SKW 6.4 cells

№	Behavior of the model by Bentele *et al.*	Behavior of the reduced model	The composite model behavior	Experimental observations by Bentele *et al.* and predictions of the models[4]
1				**Experiments by Bentele *et al.*:** − for 1 ng/ml of anti-CD95, PARP cleavage was not observed; − the measured death rate for 10 ng/ml of anti-CD95 was 20-30%. **Original and reduced models:** − the apoptotic threshold[5] is 1.9 and 6.9 ng/ml for the original and reduced models, respectively; − cPARP concentration rises dramatically within an extremely narrow interval of anti-CD95 levels overcoming the apoptotic threshold. **Composite model:** − the apoptotic threshold is 3.5 ng/ml; − cPARP concentration rises in a smooth manner along with the increase of anti-CD95 level.
2				**Experiments by Bentele *et al.*:** down-regulation of cFLIP in SKW 6.4 cells by addition of cyclohexamide resulted in cell death (40% for 1 day) already upon 1 ng/ml of anti-CD95. The level of cFLIP was decreased to 70%. **All models:** − the apoptotic threshold is highly sensitive to the concentration of cFLIP; − decreasing the initial concentration of cFLIP by more than 51%, 86% and 49% for the original, reduced and composite models, respectively, leads to cell death upon stimulation by 1 ng/ml of anti-CD95.
3				**Experiments by Bentele *et al.*:** in the 10 ng/ml activation scenario, a significant increase of caspase-8 was observed after more than 4 hours. **All models:** anti-CD95 concentrations which are slightly above the apoptotic threshold result in caspase-8 activation after a delay of many hours. The figures show peak times of caspase-8 concentration exceeding 0.1% of initial procaspase-8 level.

[4] The simulation time was 2880 min (2 days) in all predictions.

[5] The apoptotic threshold is the concentration of anti-CD95 after which cPARP amount exceeds 10% of the initial PARP level.
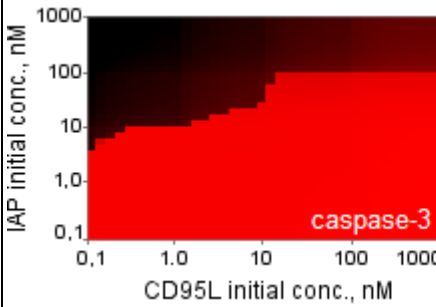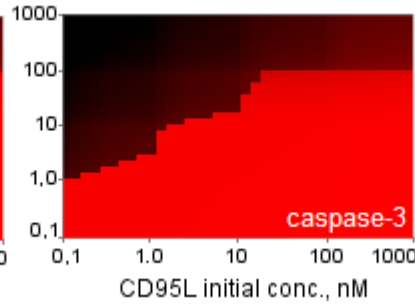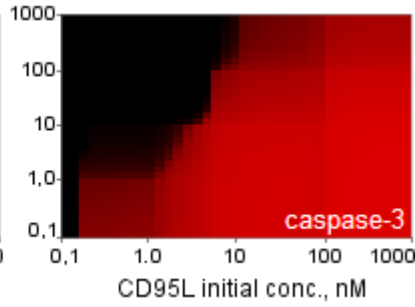
Table 9S (continuation)

№	Behavior of the model by Bentele *et al.*	Behavior of the reduced model	The composite model behavior	Experimental observations by Bentele *et al.* and predictions of the models
4				**Original and reduced models:** − low concentrations of IAP (less than 1 nM) result in complete cell death; − high concentrations of IAP prevent significant increase of caspase-3 even for high concentrations of the ligand. **Composite model:** − low concentrations of IAP (less than 1 nM) block apoptosis for CD95L less than 0.3 nM; − high concentrations of CD95L lead to cell death. The figures show logarithmic dependence of the maximal caspases-3 concentration on initial values of IAP and CD95L.

Table 10S – Parametric constraints of the models by Bentele *et al.* and Neumann *et al.*

№	Parametric constraints of the Bentele's model[6]	Corresponding reduction steps
1	$C_{casp7} \approx a \cdot C_{casp3}, \ a = const,$ $k_{7act} \cdot C_{casp7} \gg k_{36act} \cdot C_{casp3} > k_{36act} \cdot C_{casp6},$ $Km_{367act} \gg (1 - x_{aa})$	Simplification of the equation of x_{aa} production
2	$v_{br3} \approx v_{br4} \approx v_{br5} \approx v_{br6} \approx v_{br12} \approx v_{br13}$	Elimination of quasi-stationary intermediates CD95R:CD95L, DISC:pro8, DISC:pro8$_2$ and DISC:p43/p41. Removal of slow reactions br12 and br13
3	$C_{casp6} \approx b \cdot C_{casp3}, \ b = const$	Deletion of caspase-6 and procaspase-6
4	$C_{pro8} \gg Km_{68}$ or $v_{br6} \gg v_{br8}$	Formation of the linear kinetic law of caspase-8 activation triggered by caspase-3
5	$v_{br9} \approx v_{br10}$	Elimination of the quasi-stationary species DISC:cFLIPL
6	$C_{FLIPL}(0) = C_{FLIPS}(0),$ reactions br9 and br11 have the same rate constant k_{DISC_FLIP}.	Lumping of cFLIPL and cFLIPS
7	$v_{br19}, v_{casp9\ degr} \gg v_{br20}, v_{br35}, v_{br38}$	Deletion of slow reactions of apoptosome complex dissociation (br20), caspase-9 inhibition (br35) and casp9:IAP dissociation (br38)
8	$v_{br15}/(v_{br16} - vbr17) \approx const$	Elimination of cytochrome C
9	$v_{br18} \approx v_{br19}$	Elimination of the quasi-stationary apoptosome complex
10	$v_{br22} > v_{br23}$	Deletion of reaction br23 (Bid truncation) and caspase-2
11	$Km_{8Bid} \gg C_{Bid}$	Replacement of the Michaelis-Menten kinetics in br22 with the mass action kinetics
12	$v_{br27} > v_{br28},$ $v_{br29} \gg v_{br30}$	Removal of the reactions of caspase-3 (br28) and caspase-7 (br30) cleavage triggered by caspase-9
13	$v_{br27}, v_{br33}, f_{degr}(x_{aa}) \cdot C_{casp3} \gg v_{br36},$ $v_{br29}, v_{br34}, f_{degr}(x_{aa}) \cdot C_{casp7} \gg v_{br37}$	Deletion of the slow reactions of casp3:IAP (br36) and casp7:IAP (br37) dissociation
14	$v_{br33}, v_{br34} \gg v_{br25}, v_{br26}$	Taking into account the steps described above, we can get only four reactions involving IAP (br33, br34, br25 and br26). At this stage, we can remove reactions br25 and br26, as well as their members Smac and IAP:Smac.
15	$v_{br32} > v_{br31}$	Removal of the reaction of PARP cleavage by caspase-3
16	$Km_{78} \gg C_{pro7}$	Replacement of the Michaelis-Menten kinetics in br29 by the mass action kinetics
17	$Km_{367act} \gg C_{PARP},$ $C_{casp7} \approx a \cdot C_{casp3}, \ a = const$	Modification of kinetics of br32
№	Parametric constraints of the Neumann's model	Corresponding reduction steps
1	$k2 \cdot C_{pro8}, k3 \cdot C_{FLIPL} \gg k4 \cdot C_{FLIPS}$	The slow reaction of the DISC binding by FLIPS (nr4) leads to production of a very small amount of DISC:FLIPS. Therefore, all reactions involving this complex (nr4, nr11-nr13) can be removed without any significant effect on the model dynamics.
2	$C_{IKK} \gg C_{p43FLIP}$	Setting the constant value of the IKK concentration

---

[6]We did not analyze the constraints on degradation rates of species.